

Conformational Effects on Long-Range Electron Transfer: Comparison of Oligo-*p*-phenylene and Oligo-*p*-xylene Bridges

David Hanss^[a] and Oliver S. Wenger*^[a]

Keywords: Charge transfer / Donor-acceptor systems / Molecular wires / Photochemistry / Ruthenium

Phototriggered intramolecular electron transfer across variable-length oligo-*p*-phenylene and oligo-*p*-xylene bridges was investigated in seven molecules. For both types of bridges, charge transfer rates decrease exponentially with increasing number of spacer units. The distance decay parameter is 0.21 Å⁻¹ for the phenylenes and 0.77 Å⁻¹ for the xylenes. A simple analysis based on superexchange theory indicates that this difference is due to unequal electronic coupling between adjacent bridging units. On the basis of the

experimental data, phenyl-phenyl coupling is found to be roughly 7 times stronger than xylyl-xylyl coupling. This difference in electronic coupling strengths can be explained satisfactorily on the sole basis of conformational effects. It is consistent with equilibrium torsion angles of 35–40° between two phenyls and 65–70° between two xylyls.

(© Wiley-VCH Verlag GmbH & Co. KGaA, 69451 Weinheim, Germany, 2009)

Introduction

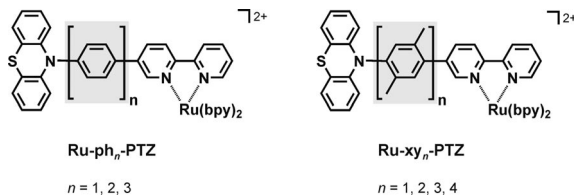
“Flatter is better” is the current credo when it comes to finding molecular wires that are capable of mediating charge transfer over several nanometers. As a matter of fact, the most efficient organic molecular wires known to date are highly π -conjugated (“flat”) systems such as oligo-*p*-phenylene vinylenes,^[1] oligo-*p*-phenylene ethynylenes,^[2] oligo-fluorenes,^[3] and oligo-*p*-phenylenes.^[4] These materials mediate long-range charge transfer far better than alkanes,^[5] peptide bridges,^[6] or ordinary protein backbone.^[7] A commonly used measure to describe the efficiency of long-range electron transfer is its distance decay parameter (β). The smaller the β value, the longer is the distance over which charge can be transferred in a given amount of time. Typical values for β are 0.01–0.1 Å⁻¹ for some of the above-mentioned π -conjugated wires,^[1a,1c,1e,3a,3b] 0.9–1.4 Å⁻¹ for non-conjugated covalent bridges,^[5,6,8] and 1.2–1.7 Å⁻¹ for charge transfer across frozen solvent matrices.^[9] However, these β values are governed by several factors that sometimes all vary at the same time when one is to compare different molecular wires with one another. One complication emerges from the fact that matching of the energy levels of the wire and the donor may affect strongly the β values.^[1a,10] In practice it can therefore be difficult to isolate the influence of conformational effects on the long-range charge transfer efficiency. Another point to consider is that for some molecular wires, the β value is reduced to a phen-

omenological parameter with little actual physical meaning because the overall donor→acceptor electron transfer is a combination of several individual electron transfer steps between adjacent bridging units.

There have been several prior studies on the influence of molecular conformation on electronic coupling across biphenyl bridging units.^[11–13] In the current work we have sought to explore conformational effects on charge transfer across longer bridges. In view of the abovementioned challenges, suitable model systems were selected according to the following criteria: (i) the molecular bridge should mediate long-range charge transfer by a single-step tunneling process, (ii) the overall wire should be comprised of a changeable number of identical units, (iii) a significant alteration in equilibrium conformation between the individual bridging units should be easily attainable, and (iv) the donors and acceptors should always be the same. On this basis we identified oligo-*p*-phenylene and oligo-*p*-xylene molecules as promising bridges. The equilibrium torsion angle between adjacent *p*-xylene units is substantially greater than that between two neighboring phenyl moieties due to steric hindrance.^[4f,14] Length variation is synthetically viable for both types of bridges,^[15] and they can both be attached relatively easily to common donors and acceptors.^[14,16] Our choice fell upon a ruthenium(II) tris(2,2'-bipyridine) complex [Ru(bpy)₃]²⁺ as a photosensitizer and a phenothiazine (PTZ) as an electron donor, because phototriggered charge transfer between these two redox partners produces clear-cut spectroscopic signatures.^[17–21] In prior work we have already investigated phototriggered charge tunneling across oligo-*p*-xylene bridges,^[14,22] amongst others in the Ru-xy_{*n*}-PTZ molecules from Scheme 1.^[23] Here, we report on a similar investigation of

[a] University of Geneva, Department of Inorganic, Analytical and Applied Chemistry, 30 Quai Ernest-Ansermet, 1211 Geneva 4, Switzerland
Fax: +41-22-3796069
E-mail: oliver.wenger@unige.ch

oligo-*p*-phenylene bridged systems (Ru-ph_{*n*}-PTZ). Comparison of the phenylene and xylene charge transfer data provides direct insight into the importance of conformational effects on long-range charge transfer.



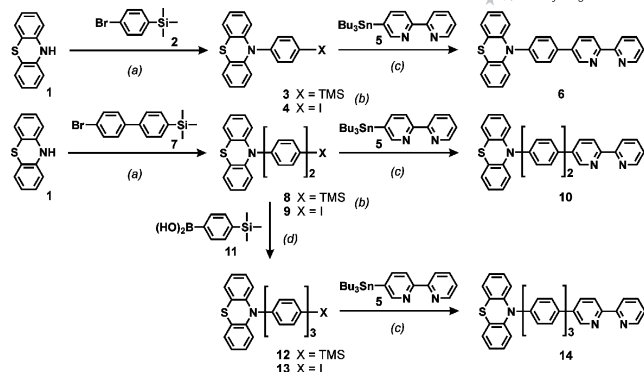
Scheme 1. The molecules investigated in this work (bpy = 2,2'-bipyridine).

Results and Discussion

Synthesis of Phenothiazine-Phenylene-Bipyridine Ligands

The most important part in the synthesis of the molecules from Scheme 1 is the synthesis of phenothiazine-bridge-bipyridine ligands as illustrated in Scheme 2 for the oligo-*p*-phenylene systems. Five different molecular building blocks are necessary for this: Phenothiazine (**1**) (commercially available), (4-bromophenyl)trimethylsilane (**2**) (accessible in one step from buyable 1,4-dibromobenzene),^[14,15,24] 5-(tri-*n*-butylstannyl)-2,2'-bipyridine (**5**) (made in 3 steps from the commercial chemicals 2-bromopyridine and 2,5-dibromopyridine),^[25] 4-bromo-4'-(trimethylsilyl)biphenyl (**7**) (available in one step from the buyable 4,4'-dibromo compound),^[14] and 4-trimethylsilylphenylboronic acid **11** (synthesized in two steps from 1,4-dibromobenzene).^[14,15,24] With these building blocks at hand, the desired ligands are accessible in acceptable yields using only four different reaction types: (a) a palladium(0)-catalyzed N–C coupling to attach the phenothiazine to the phenylene bridges,^[26] (b) a trimethylsilyl (TMS)–iodo exchange to deprotect and activate the coupling product for further cross-coupling reactions,^[15] (c) coupling of the iodo species to the 2,2'-bipyridine (bpy) ligand using a Stille methodology, and (d) lengthening of the bridge in a Suzuki-type C–C coupling reaction. Reactions (a), (b), (d) all proceed with satisfactory yields [typically superior to 60 percent for (a) and (b), and 80% for (d)]. Substantially lower yields (23% to 54%) result for the Stille couplings (d). We have sought to replace stannane **5** by the corresponding boronic acid or its pinacol ester, but our own attempts to synthesize any of these building blocks following an existing synthetic protocol have so far been unsuccessful.^[27] Global yields for the final ligands from Scheme 2 are 48% (**6**), 20% (**10**), and 7% (**14**).

The synthesis of the analogous *p*-xylene-bridged phenothiazine-bipyridine ligands has been previously reported by us.^[23] Briefly, it follows an identical synthetic strategy, only with methylated analogs of building blocks **2**, **7**, and **11**. An important difference between the phenylene- and xylene-bridged molecules concerns their solubility. Tri-*p*-phenylene molecule **13** is already rather poorly soluble in all common organic solvents even at elevated temperatures. Its coupling



Scheme 2. Synthesis of the phenothiazine-(oligo-*p*-phenylene)-bipyridine ligands needed for the Ru-ph_{*n*}-PTZ molecules: (a) Pd(dba)₂, P(*t*Bu)₃, *t*BuOK, toluene (60 °C); (b) ICl, CH₃CN/CH₂Cl₂ (3:1, 25 °C); (c) Pd(PPh₃)₄, *m*-xylene (reflux); (d) Pd(PPh₃)₄, Na₂CO₃, toluene/ethanol/water (85:10:5, reflux).

to bipyridine **5** and subsequent (column chromatography) purification of the desired coupling product **14** from undesired byproducts is still possible, but for the tetra-*p*-phenylene congener this is not the case any more. We are thus limited to a bridge length comprised of three phenyl units, whereas for the *p*-xylene bridges solubility was no issue up to *n* = 4. It is plausible that intermolecular stacking interactions are responsible for the lower solubility of the phenylene molecules: oligo-*p*-phenylenes adopt more planar equilibrium conformations than oligo-*p*-xylenes (see below), and this may favor formation of aggregates through π - π interactions.

Complexation of the ligands from Scheme 2 to ruthenium is a synthetically trivial matter: Ru(bpy)₂Cl₂ precursor is reacted with **6**, **10**, or **14** in ethanol/chloroform mixtures at reflux,^[28] whereby the target molecules (Ru-ph_{*n*}-PTZ) are obtained.

π -Conjugation Effects

Figure 1 shows the optical absorption spectra of the Ru-ph_{*n*}-PTZ and Ru-xy_{*n*}-PTZ molecules from Scheme 1 in acetonitrile solutions at room temperature. Three absorption bands are easily noticeable in all seven spectra, notably the ruthenium(II)-to-bipyridine metal-to-ligand charge transfer (MLCT) band at ca. 460 nm, a bpy-localized π - π^* band at ca. 290 nm, and a band around 260 nm that is due to a PTZ-localized electronic transition.^[23] A fourth absorption band is noticeable as a detached band only in the Ru-ph₂-PTZ and Ru-ph₃-PTZ molecules with maxima at 320 nm and 330 nm, respectively. In all other spectra, notably in those of all Ru-xy_{*n*}-PTZ molecules, it merely appears as a shoulder to the above-mentioned bpy π - π^* band. For both types of molecular bridges, this absorption red-shifts with increasing number of bridging units, and it does so more than any other absorption band. Thus it appears plausible to assign these absorption bands to predominantly bridge-localized electronic transitions.^[29]

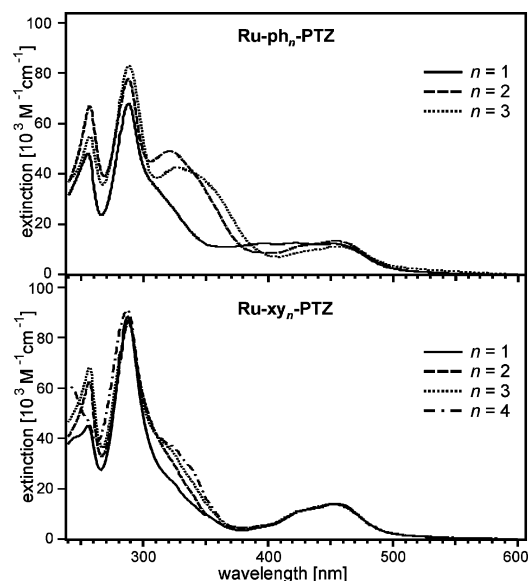


Figure 1. Optical absorption spectra of the molecules from Scheme 1 in acetonitrile solution at room temperature.

The observed red-shifts are consistent with increasing π -conjugation with increasing length – an effect which is expected to be more important for the oligo-*p*-phenylenes than for the oligo-*p*-xylenes due to steric reasons.^[4f] Interphenyl torsion angles are of the order of 35° (calculated gas-phase structures) which implies substantial π -conjugation across adjacent phenyls.^[4c,30] Analogous calculations on oligo-*p*-xylene molecules (see below) indicate that interxylyl equilibrium torsion angles are closer to 70° , angle at which the overlap between p_z -orbitals from neighboring xylyls is substantially smaller. This data interpretation is in line with that from recent work on similarly substituted oligo-*p*-phenylene wires.^[4f] Analogous experimental observations have also been made in our prior work on *p*-xylene and *p*-phenylene bridged rhenium(I)-phenothiazine systems.^[14,22]

Excited-State Quenching Due to Electron Transfer in the Ru-ph_n-PTZ Molecules

When acetonitrile solutions of the molecules from Scheme 1 are excited into the Ru^{II}→bpy ¹MLCT band at 450 nm, the emission spectra in Figure 2 are observed. The shapes and the energetic positions of the luminescence bands are virtually identical to those of the free Ru(bpy)₃²⁺ complex. On this basis we assign the luminescence in our Ru-ph_n-PTZ and Ru-xy_n-PTZ molecules to the same ³MLCT emission as observed for the reference complex. Significant differences in emission intensities are observed between Ru-ph_n-PTZ molecules of different bridge length: The shorter the bridge, the weaker the luminescence signal is. The Ru-xy_n-PTZ molecules, by contrast, exhibit bridge-length independent luminescence intensities. Time-resolved luminescence experiments are consistent with the results from steady-state emission spectroscopy: in freeze-pump-

thaw deoxygenated acetonitrile solution, all Ru-xy_n-PTZ luminescence lifetimes are between 828 and 861 ns (Table 1), whereas that of the free Ru(bpy)₃²⁺ complex is 865 ns under identical experimental conditions. The Ru-ph_n-PTZ emission lifetimes are 139 ns ($n = 3$), 75 ns ($n = 2$), 30 ns ($n = 1$). Thus it is obvious that an excited-state quenching process is at work in the Ru-ph_n-PTZ molecules that is inactive in the Ru-xy_n-PTZ systems. There exist numerous reports on reductive quenching of the Ru(bpy)₃²⁺ ³MLCT state by phenothiazine.^[17,19,20,31] However, the driving-force associated with PTZ→*Ru(bpy)₃²⁺ electron transfer is usually very low, and therefore in certain instances this process is inefficient and little to no luminescence quenching is observable.^[32] We have previously used this argument to explain the absence of quenching in the Ru-xy_n-PTZ molecules.^[23a] Now, for the Ru-ph_n-PTZ systems, such quenching is observed, suggesting that PTZ→*Ru(bpy)₃²⁺ excited-state electron transfer is more exergonic in these new molecules.

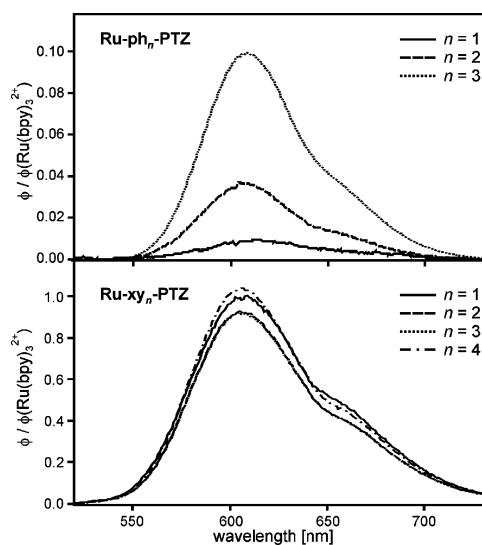


Figure 2. Luminescence spectra of the molecules from Scheme 1 in acetonitrile solution at room temperature. Excitation occurred at 450 nm; the optical density at this wavelength was 0.10 for all samples.

This driving-force issue can be addressed with electrochemical experiments. The cyclic voltammograms in Figure 3 were obtained from acetonitrile solutions of Ru-ph₁-PTZ and Ru-xy₁-PTZ molecules in presence of a ferrocene (Fc) reference and tetrabutylammonium hexafluorophosphate electrolyte. One observes the typical waves associated with bpy reduction (ca. -1.2 V vs. SCE), PTZ oxidation (ca. $+0.75$ V vs. SCE), and Ru^{II} oxidation (ca. 1.25 V vs. SCE). The values given here and in Table 2 are half-wave potentials ($E_{1/2}$), but in Figure 3 we show four vertical dashed lines that mark the positions of oxidation wave maxima. This makes the following interesting observation more obvious: PTZ oxidation occurs at a less positive potential in Ru-ph₁-PTZ than in Ru-xy₁-PTZ, the difference in $E_{1/2}$ values is 70 mV. It appears tempting to attribute the discrepancy in redox potentials to differences in π -conjugation, after all

Table 1. Donor-acceptor distances (r_{DA}), luminescence quantum yields (ϕ_{lum}) relative to $Ru(bpy)_3^{2+}$, MLCT luminescence lifetimes (τ_{MLCT}), rate constants for intramolecular (thermal) charge recombination (k_{CR}) between $Ru(bpy)_3^{3+}$ and PTZ^+ in the $Ru-ph_n$ -PTZ molecules, and rate constants for intramolecular PTZ -to- Ru^{III} - $(bpy)_3^{3+}$ ground-state electron transfer ($k_{ET,gs}$) in the $Ru-xy_n$ -PTZ molecules. All measurements were made in acetonitrile solution.

	r_{DA} [Å]	$\phi_{lum}^{[a]}$	τ_{MLCT} [ns] ^[b]	k_{CR} [s ⁻¹] ^[b]	$k_{ET,gs}$ [s ⁻¹] ^[b]
Ru-ph ₁ -PTZ	10.6	0.01	30	6.9×10^7	
Ru-ph ₂ -PTZ	14.9	0.04	75	2.3×10^7	
Ru-ph ₃ -PTZ	19.2	0.10	139	1.1×10^7	
Ru-xy ₁ -PTZ	10.6	0.92	842		$\geq 10^8$
Ru-xy ₂ -PTZ	14.9	0.87	828		3.8×10^7
Ru-xy ₃ -PTZ	19.2	0.85	861		7.1×10^5
Ru-xy ₄ -PTZ	23.5	0.95	855		4.9×10^4
$[Ru(bpy)_3]^{2+}$		1.00	865		

[a] Relative to $[Ru(bpy)_3]^{2+}$. [b] In freeze-pump-thaw deoxygenated acetonitrile.

the PTZ - ph torsion angle is expected to be significantly lower than the PTZ - xy dihedral angle for steric reasons. However, we also note that the uncertainty associated with our experimental redox potentials is on the order of ± 0.05 V. The absorption (Figure 1) and luminescence spectra (Figure 2) indicate that the energy of the emissive ³MLCT state is the same in all seven molecules from Scheme 1. From the similarity of these spectra to those of the $Ru(bpy)_3^{2+}$ reference complex we assume an identical ³MLCT energy of $E_{00} = 2.12$ eV.^[33] This leads to an estimated potential of roughly 0.9 V vs. SCE for one-electron reduction of photoexcited $Ru(bpy)_3^{2+}$ for all $Ru-ph_n$ -PTZ and $Ru-xy_n$ -PTZ molecules. In first approximation,^[34] this yields the following reaction free energies: $-\Delta G_{ET,xy} \approx 0.11$ eV for $Ru-xy_n$ -PTZ and $-\Delta G_{ET,ph} \approx 0.18$ eV for $Ru-ph_n$ -PTZ based on the $E_{1/2}$ values in Table 2. Given the approximate nature of these calculated $-\Delta G_{ET}$ values and the experimental uncertainty associated with the redox potentials obtained from cyclic voltammetry, it would be daring to draw more quantitative conclusions than to state that both excited-state electron transfers have very small driving forces. We are thus forced to accept it as a simple fact that (for kinetic reasons) excited-state electron transfer *is* observed for the $Ru-ph_n$ -PTZ molecules but *not* for the $Ru-xy_n$ -PTZ dyads.

Direct experimental evidence for excited-state electron transfer in the $Ru-ph_n$ -PTZ molecules comes from transient absorption spectroscopy. The spectrum shown in Figure 4 was measured on a 2×10^{-5} M sample of $Ru-ph_1$ -PTZ in deoxygenated acetonitrile; the data was acquired in a 100-ns time window starting 30 ns after the 457.9-nm excitation pulse. The positive signal around 380 nm can be attributed to a one-electron reduced bpy ligand ($bpy^{\cdot-}$),^[32,35] whereas the bleach between 400 and 480 nm is due to the disappearance of Ru^{II} .^[23,32] The positive signal between 480 and 550 nm can be assigned to overlapping absorptions from $[Ru(bpy)_3]^+$ and phenothiazine radical cation ($PTZ^{\cdot+}$).^[18–20] From prior work it is known that the molar extinction coefficient of $Ru(bpy)_3^+$ at 510 nm is a factor of 2 greater than that of $PTZ^{\cdot+}$ at the same wavelength ($\epsilon_{Ru^+,510} =$

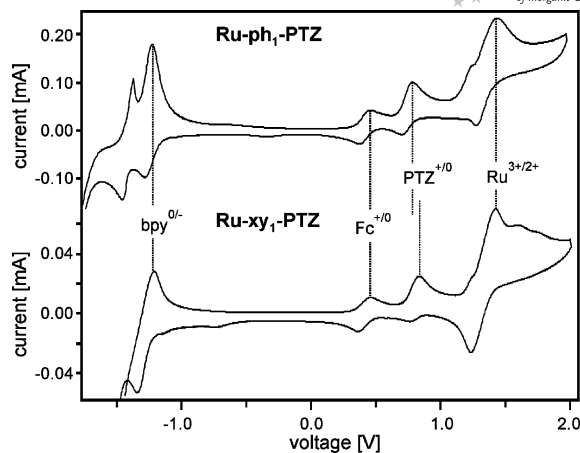


Figure 3. Cyclic voltammograms for the mono-*p*-phenylene and mono-*p*-xylene bridged dyads in acetonitrile solution using tetrabutylammonium hexafluorophosphate as supporting electrolyte. The dashed vertical lines mark oxidation peak potentials, but the values given in Table 1 are half-wave potentials.

Table 2. Half-wave redox potentials (E) of the dyads and two reference molecules, measured in acetonitrile solution at room-temperature using an $Ag/AgCl$ quasi-reference electrode, but reported vs. SCE.

	$E(Ru\{bpy\}_3^{2+/+})$ [V vs. SCE]	$E(Ru\{bpy\}_3^{3+/2+})$ [V vs. SCE]	$E(PTZ^{+/0})$ [V vs. SCE]
Ru-ph ₁ -PTZ	-1.22	1.24	0.72
Ru-ph ₂ -PTZ	-1.25	1.23	0.70
Ru-ph ₃ -PTZ	-1.24	1.23	0.72
Ru-xy ₁ -PTZ	-1.22	1.22	0.79
Ru-xy ₂ -PTZ	-1.22	1.26	0.75
Ru-xy ₃ -PTZ	-1.17	1.21	0.80
Ru-xy ₄ -PTZ	-1.27	1.17	0.73
$[Ru(bpy)_3]^{2+}$	-1.28	1.26	
10-(<i>p</i> -xylyl)-PTZ			0.79

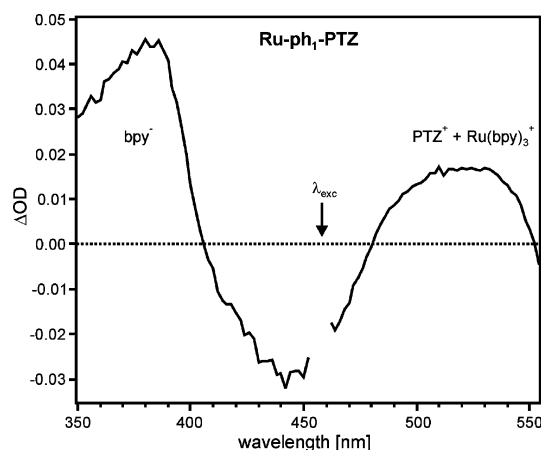


Figure 4. Transient absorption spectrum measured on a 2×10^{-5} M solution of $Ru-ph_1$ -PTZ in freeze-pump-thaw deoxygenated acetonitrile. Excitation occurred at 457.9 nm with 10-ns laser pulses (λ_{exc}), and the signal was detected during a 100-ns time window starting 30 ns after the pulse.

$10'000 \text{ M}^{-1} \text{ cm}^{-1}$, $\epsilon_{PTZ^+,510} = 5'000 \text{ M}^{-1} \text{ cm}^{-1}$).^[18,32,36,37] This explains why the Ru-ph₁-PTZ transient absorption band between 480 and 550 nm reflects more the symmetrical bandshape of the Ru(bpy)₃²⁺ signal than that of the more asymmetrical PTZ⁺ absorption.^[18–20] Analogous transient absorption spectra were obtained for the longer congeners of the Ru-ph_{*n*}-PTZ molecules (*n* = 2 or 3), but for the Ru-xy_{*n*}-PTZ molecules no such transient absorption bands can be observed. In short, PTZ-to-Ru^{II} excited-state electron transfer occurs in the Ru-ph_{*n*}-PTZ molecules but not in the Ru-xy_{*n*}-PTZ systems.

There is no evidence for triplet-triplet energy transfer from the photoexcited metal center to the phenylene or xylene bridges. This is not surprising since the lowest-energetic triplet state in terphenyl is at $\geq 2.5 \text{ eV}$,^[29] that is energetically well above the ³MLCT state of Ru(bpy)₃²⁺ ($E_{00} = 2.12 \text{ eV}$). The shorter phenylene bridges have even higher triplet energies.

Kinetics of Charge Transfer in the Ru-ph_{*n*}-PTZ Molecules

The right column of Figure 5 shows the temporal evolution of the transient absorption signals at 510 nm of the three Ru-ph_{*n*}-PTZ molecules in deoxygenated acetonitrile solution. For a given dyad, the kinetic trace obtained is practically identical to that measured for the luminescence signal at 650 nm (left column in Figure 5).

The same observation has been made previously for a covalently linked Ru(bpy)₃²⁺-PTZ donor-acceptor couple. A recent study demonstrated that the establishment of a quasi-equilibrium between the Ru ³MLCT state and the Ru(bpy)₃²⁺-PTZ⁺ charge-separated state (Scheme 3) can

account for this behavior.^[32] Due to the close energetic proximity of these two states in our Ru-ph_{*n*}-PTZ molecules (see above), the possibility of a quasi-equilibrium must be considered. Direct experimental evidence for this phenomenon can be obtained from the transient absorption data, since the two electronic states in question have different spectra: at 510 nm, ³MLCT-excited Ru(bpy)₃²⁺ absorbs only very weakly ($\epsilon_{MLCT} < 500 \text{ M}^{-1} \text{ cm}^{-1}$),^[35] but the Ru(bpy)₃²⁺-PTZ⁺ charge-separated state produces a strong absorption at this wavelength ($\epsilon_{Ru^+,510} + \epsilon_{PTZ^+,510} = 15'000 \text{ M}^{-1} \text{ cm}^{-1}$; see above).^[18,36,37] At 370 nm, both states have the same extinction ($\epsilon_{bpy,370} = 20'000 \text{ M}^{-1} \text{ cm}^{-1}$) because the absorption at this wavelength is due to a one-electron reduced bpy ligand that is formed in both cases: MLCT excitation produces a Ru^{III}(bpy)₂(bpy⁻) state, whereas the charge-separated state can be described as Ru^{II}(bpy)₂(bpy⁻)-PTZ⁺.^[35] Consequently, for the charge-separated state, one expects an intensity ratio of 4:3 for the transient absorption signals at 370 nm and 510 nm, respectively. Our experimental observation is that these ratios are about 8:3 for all Ru-ph_{*n*}-PTZ molecules (Figure 4), suggesting that the Ru ³MLCT and the Ru(bpy)₃²⁺-PTZ⁺ charge-separated state are populated each to about 50%. This in turn implies that PTZ→*Ru(bpy)₃²⁺ excited-state electron transfer is nearly isoergonic in the Ru-ph_{*n*}-PTZ molecules, as suspected above.

The experimentally observed emission and transient absorption decays (Figure 5) are single exponential and yield lifetimes of 30 ns (*n* = 1), 75 ns (*n* = 2), and 139 ns (*n* = 3) as summarized in Table 1. In the quasi-equilibrium, the experimentally accessible decay rate constant k_{obs} is a function of the intrinsic ³MLCT excited-state decay rate constant k_{MLCT} (which itself contains a radiative and a nonra-

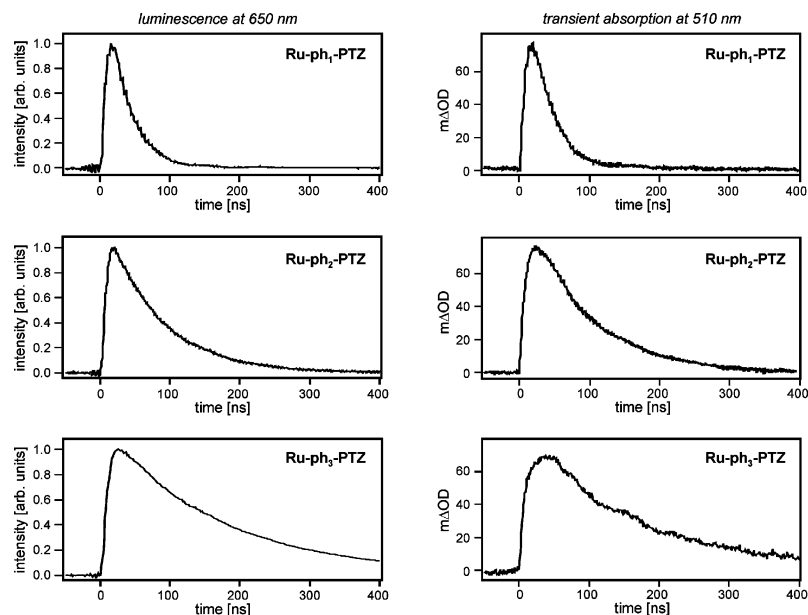
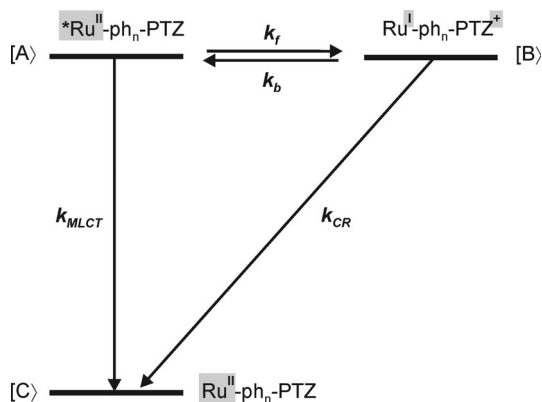


Figure 5. Left: decays of the luminescence signals in the Ru-ph_{*n*}-PTZ molecules after pulsed excitation of $2 \times 10^{-5} \text{ M}$ (deoxygenated) acetonitrile solutions at 457.9 nm with laser pulses of about 10 ns duration. Right: temporal evolution of the Ru-ph_{*n*}-PTZ transient absorption signals from Figure 4 with a detection wavelength of 510 nm.



Scheme 3. Energy level scheme for the Ru-ph_n-PTZ molecules. The close energetic proximity of the Ru ³MLCT ([A]) and the Ru(bpy)₃⁺-PTZ⁺ charge-separated state ([B]) leads to a quasi-equilibrium situation (k_f , k_b) between these two states.

diative part) and the rate constant k_{CR} for decay of the Ru(bpy)₃⁺-PTZ⁺ charge-separated state to the ground state:

$$k_{obs} = \frac{N_{MLCT}}{N_{MLCT} + N_{CS}} k_{MLCT} + \frac{N_{CS}}{N_{MLCT} + N_{CS}} k_{CR} \quad (1)$$

where N_{MLCT} and N_{CS} represent the population numbers of the ³MLCT and charge-separated states, respectively. The numerical value of k_{MLCT} for all three Ru-ph_n-PTZ molecules can be set equal to the inverse of the luminescence lifetime of free Ru(bpy)₃²⁺ in reasonable approximation. Thus, with $k_{MLCT} = 1.2 \times 10^6 \text{ s}^{-1}$ (Table 1) and $N_{CS} = N_{MLCT} = 0.5$ (see above), one obtains the charge-recombination rate constants listed in the fourth column of Table 1: $k_{CR} = 6.9 \times 10^7 \text{ s}^{-1}$ for $n = 1$, $k_{CR} = 2.3 \times 10^7 \text{ s}^{-1}$ for $n = 2$, and $k_{CR} = 1.1 \times 10^7 \text{ s}^{-1}$ for $n = 3$. As pointed out earlier,^[32] there exist analytical expressions that put the rise and decay of the transients into relation with the rate constants k_f and k_b (Scheme 3) governing the kinetics of the equilibration process. This analysis yields $k_f = 4.9 \times 10^7 \text{ s}^{-1}$ for each of the three Ru-ph_n-PTZ molecules, due to the fact that our rise kinetics are limited by the experimental setup used for these experiments. Thus, it is impossible to extract meaningful values for k_f (and k_b) from our data, but it is clear that $k_f = 4.9 \times 10^7 \text{ s}^{-1}$ represents a lower limit for the rate of *Ru(bpy)₃²⁺ → PTZ excited-state electron transfer; the equilibration process must be rapid with respect to the decays of the ³MLCT state and the charge-separated state.

Steady state luminescence experiments show that the emission intensity of the Ru-ph₃-PTZ molecule is ca. 10% of that emitted by the free Ru(bpy)₃²⁺ reference complex (Table 1). This is in good agreement with estimates based on the above kinetic data: the amount of the quasi-equilibrium population decaying from the ³MLCT state is represented by the first summand in Equation (1). Its division through k_{obs} gives a calculated quantum yield $\phi_{calc,ph3} = 0.083$ relative to Ru(bpy)₃²⁺. Similarly good agreement between experimental and calculated relative emission quantum yields is obtained for the shorter Ru-ph_n-PTZ mole-

cules. For $n = 2$, $\phi_{exp} = 0.04$ and $\phi_{calc} = 0.045$, whereas for $n = 1$, $\phi_{exp} = 0.01$ and $\phi_{calc} = 0.018$ (Table 1).

The quasi-equilibrium scenario is also consistent with the absolute magnitudes of the experimentally observed ΔOD values in the transient absorption experiments (Figure 4 and Figure 5): the extinction of the charge-separated state at 510 nm is $15'000 \text{ M}^{-1} \text{ cm}^{-1}$ (see above),^[18,36,37] the concentrations of our solutions were $2 \times 10^{-5} \text{ M}$. If 20% of the Ru-ph_n-PTZ molecules are excited and 50% of them populate the charge-separated state, this yields $\Delta OD_{510} = 0.03$, which compares favorably to our experimental values that are of the order of $\Delta OD_{510} = 0.02$ to 0.07 . This point is noteworthy because it rules out a hypothetical scenario in which $k_{CR} \gg k_f$. Numerical simulations based on a set of coupled differential equations for a simple three-level scheme demonstrate that the decays of the transients in Figure 5 can also be reproduced when k_{CR} values exceed those for k_f by roughly two orders of magnitude. This finding is captured also by an analytical expression describing the population of intermediate B in a reaction sequence $A \rightarrow B \rightarrow C$:^[38] Under the condition that the rate constant for transformation of B to C (k_{bc}) is much greater than that for transformation of A to B (k_{ab}), the concentration of B is given by:^[38]

$$[B] = \frac{k_{ab}}{k_{bc}} [A]_0 \exp(-k_{ab}t) \quad (2)$$

where $[A]_0$ represents the initial concentration of starting material A. As seen from Equation (2), the decay is characterized by k_{ab} , suggesting that the transient absorption decay in Figure 5 could be associated with k_f , that is with the charge-separation process. However, the first factor in the analytical Equation (2) anticipates a result that also emerges from the abovementioned numerical simulations, namely that under these circumstances the maximum population of B (or in our case of the charge-separated state) is about 1/100 of the initial population of A. One would thus expect ΔOD values smaller than 0.001, which cannot be conciliated with experiment.

Distance Dependence of Charge Transfer in Ru-ph_n-PTZ and Ru-xy_n-PTZ

When the natural logarithms of the rate constants for Ru(bpy)₃⁺ → PTZ⁺ electron transfer (k_{CR}) in the Ru-ph_n-PTZ molecules (Table 1) are plotted as a function of donor-acceptor (center-to-center) distance r_{DA} , the three data points fall onto a single line (open circles in Figure 6). Such exponential distance dependences of charge transfer rates are typical of the superexchange mechanism in which the charge carrier, either an electron or a hole, must tunnel through the barrier imposed by the bridging medium.^[7a] The rate constant for charge tunneling is therefore a function of only two parameters, namely the rate constant for charge transfer for a situation in which the donor and the acceptor are in van der Waals contact (k_0) and the distance decay parameter β :^[7a]

$$k_{\text{tunnel}}(r_{DA}) = k_0 \cdot \exp(-\beta \cdot r_{DA})$$

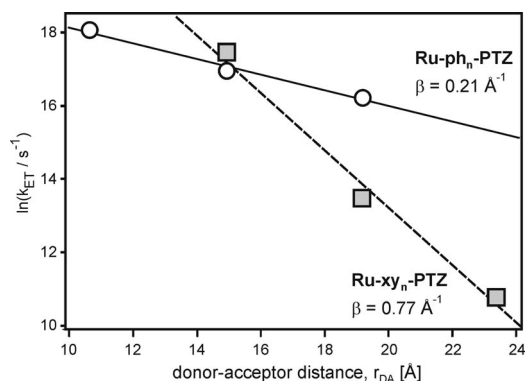


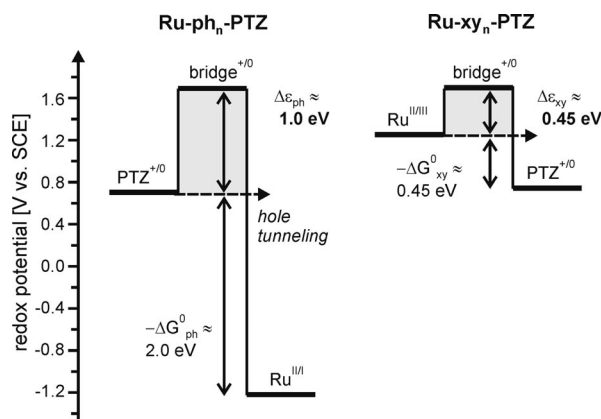
Figure 6. Distance dependence of hole tunneling from PTZ^{+} to $\text{Ru}(\text{bpy})_3^{2+}$ across oligo-*p*-phenylene bridges (open circles) and hole tunneling from photogenerated $\text{Ru}(\text{bpy})_3^{3+}$ to PTZ across oligo-*p*-xylenes (gray filled squares). The lines are linear regression fits, their slopes correspond to the distance decay parameters (β values) for the phenylene and xylene systems.

In applying Equation (3) to analysis of the electron transfer rate distance dependence, one neglects the distance dependence of all nuclear factors contributing to electron transfer rates, which corresponds to the standard approximation in the field.^[1–11] Estimates for k_0 and β for the $\text{Ru-ph}_n\text{-PTZ}$ system can be obtained from a linear regression fit to the three data points in Figure 6. Assuming $r_{DA} = 6 \text{ \AA}$ for free $\text{Ru}(\text{bpy})_3^{2+}$ and PTZ molecules in van der Waals contact, one obtains $k_0 = 1.8 \times 10^8 \text{ s}^{-1}$. For driving-force-optimized charge transfer between two reactants that are in direct contact, rate constants can be as large as 10^{13} s^{-1} .^[7a] The comparatively small value found here for the $\text{Ru}(\text{bpy})_3^{2+}/\text{PTZ}^{+}$ donor-acceptor couple is a manifestation of the fact that this thermal charge recombination process is far from driving-force-optimized.^[32] Roughly 2 eV must be liberated during this process, and it is therefore plausible that it is associated with a significant activation barrier such as the case for charge-recombination in rhenium(I)/PTZ systems for which the occurrence of an inverted driving-force effect has long been reported.^[39] More significant for the present work is the slope of the linear regression fit which yields $\beta = 0.21 \text{ \AA}^{-1}$. This value is at the lower end of what has been reported previously for charge transfer across oligo-*p*-phenylene bridges: prior investigations have produced β values ranging from 0.35 \AA^{-1} to 0.67 \AA^{-1} for tunneling through such bridges.^[4,40] For tetra- and penta-*p*-phenylene spacers, hopping processes with much weaker distance dependences were observed.^[4c] However, from recent work it is clear that β is not solely dependent on the bridge.^[10] Instead, it is a function of the entire donor-bridge-acceptor system,^[41] hence our interest in a comparison of oligo-*p*-phenylene and oligo-*p*-xylene bridges attached to the same donor and acceptor.

In the $\text{Ru-xy}_n\text{-PTZ}$ molecules there is no $\text{Ru}(\text{bpy})_3^{2+} \rightarrow \text{PTZ}$ excited-state electron transfer (see above),^[23a] and it is therefore impossible to study the distance dependence of the same charge recombination reaction as observed for the

$\text{Ru-ph}_n\text{-PTZ}$ molecules. Instead, charge tunneling across the oligo-*p*-xylene bridges was studied using a bimolecular flash-quench technique with methylviologen, whereby a highly oxidizing $\text{Ru}(\text{bpy})_3^{3+}$ species can be generated.^[23] It is then possible to investigate intramolecular $\text{PTZ} \rightarrow \text{Ru}^{\text{III}}$ electron transfer.^[32,42] The distance dependence of this process is shown by the gray-filled squares in Figure 6, and the numerical values for the electron transfer rate constants are given in the last column of Table 1. From a linear regression fit to these data we obtained $\beta = 0.77 \text{ \AA}^{-1}$.^[23a] Attempts to investigate the kinetics of the same $\text{PTZ} \rightarrow \text{Ru}^{\text{III}}$ electron transfer in the $\text{Ru-ph}_n\text{-PTZ}$ molecules were unsuccessful due to the rapidity of this process in these systems. There are both inherent physical and experimental limits on the time resolution for such investigations: ca. 1 ns for generation of Ru^{III} via bimolecular electron transfer with methylviologen,^[42] and ca. 10 ns for the laser equipment used in this work. The ca. 10 ns experimental limit precluded measurement of the $\text{PTZ} \rightarrow \text{Ru}^{\text{III}}$ charge transfer kinetics even for the $\text{Ru-ph}_3\text{-PTZ}$ molecule.^[43] The significance of this is that despite the close chemical resemblance of the two dyad series in Scheme 1, two different charge transfer processes are actually observed and compared to one another.

For both bridges, a hole tunneling mechanism is expected to prevail since the one-electron oxidized bridge levels are energetically much closer to the donor/acceptor levels than the one-electron reduced bridge states.^[33] As illustrated in Scheme 4, in the $\text{Ru-ph}_n\text{-PTZ}$ molecules there is hole tunneling from PTZ^{+} to $\text{Ru}(\text{bpy})_3^{2+}$, whereas in the $\text{Ru-xy}_n\text{-PTZ}$ systems there is Ru^{III} to PTZ hole tunneling. The energy levels in Scheme 4 were estimated from the redox potentials of all relevant species (Table 2); the bridge potential comes from a prior electrochemical study of the 4,4'-dimethyldiphenyl (dmdp) molecule.^[44] It has not been possible to measure the oligo-*p*-phenylene and oligo-*p*-xylene bridge redox potentials directly by cyclic voltammetry, but dmdp represents a reasonable approximation to the real bridges in our dyads. The dmdp molecule is oxidized at +1.67 V vs. SCE and reduced at -2.60 eV ,^[44] hence the preference for hole over electron tunneling.

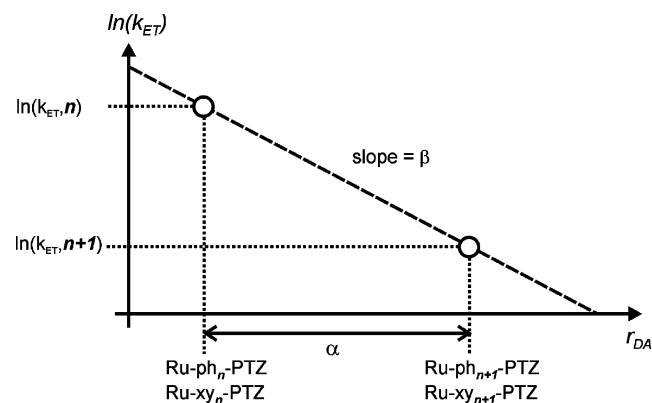


Scheme 4. Energy level diagram for hole tunneling from PTZ^{+} to $\text{Ru}(\text{bpy})_3^{2+}$ through oligo-*p*-phenylene bridges (left) and for hole tunneling from photogenerated $\text{Ru}(\text{bpy})_3^{3+}$ to PTZ across oligo-*p*-xylenes (right).

The barriers and driving-forces associated with the two hole tunneling processes in Scheme 4 differ quite significantly. According to superexchange theory, bridge-mediated donor-acceptor couplings H_{DA} are a sensitive function of the barrier height $\Delta\varepsilon$:^[7a,41,45]

$$H_{DA} = \frac{h_{Db}}{\Delta\varepsilon} \left(\frac{h_{bb}}{\Delta\varepsilon} \right)^{n-1} \cdot h_{bA} \quad (4)$$

In the strict sense of this model, $\Delta\varepsilon$ is defined as the energy difference between the donor-acceptor system at its transition state configuration and the energy levels of the bridge. Since this quantity cannot be extracted easily from experiment, it has become common to approximate $\Delta\varepsilon$ as the difference in donor and bridge redox potentials, as done in Scheme 4. The other parameters that affect H_{DA} in this model are the electronic couplings between adjacent molecular units, specifically: donor-bridge coupling (h_{Db}), bridge-bridge (h_{bb}), and bridge-acceptor (h_{bA}) coupling. The distance dependence of H_{DA} shows up in the exponent $n - 1$, wherein n represents the number of (identical) bridging units. According to semiclassical theory, electron transfer rate constants k_{ET} are proportional to H_{DA}^2 ,^[46] and their distance dependence is essentially governed by that of H_{DA} .^[7a,46] This allows us to set the experimentally determined distance decay constant β into relation with the superexchange parameters from Equation (4).



Scheme 5. Graphical illustration of the definition of the distance decay parameter β and its relation to electron transfer rate constants k_{ET} and the length (a) of a phenylene or xylene molecular unit.

From Scheme 5, it follows that

$$\beta = [\ln(k_{ET,n}) - \ln(k_{ET,n+1})]/a \quad (5)$$

where a is the length of a phenylene or xylene bridging unit (4.3 Å). With $k_{ET} \propto H_{DA}^2$ and Equation (4), Equation (5) simplifies to Equation (6).

$$\beta = \frac{2}{a} \ln \left(\frac{\Delta\varepsilon}{h_{bb}} \right) \quad (6)$$

Thus, β is a function of only three parameters (a , $\Delta\varepsilon$, h_{bb}). Notably, it is independent of the reaction free energy $-\Delta G_{ET}$. From the experimental β values (Figure 6) and the

estimated barrier heights (Scheme 4) it is now possible to estimate the relative magnitudes of phenyl-phenyl ($h_{bb,ph}$) and xylyl-xylyl coupling ($h_{bb,xy}$):

$$\frac{h_{bb,ph}}{h_{bb,xy}} = \frac{\Delta\varepsilon_{ph}}{\Delta\varepsilon_{xy}} \exp \left[\frac{a}{2} (\beta_{xy} - \beta_{ph}) \right] \quad (7)$$

With the numerical values from above ($\Delta\varepsilon_{ph} = 1.0$ eV, $\Delta\varepsilon_{xy} = 0.45$ eV, $a = 4.3$ Å, $\beta_{xy} = 0.77$ Å⁻¹, $\beta_{ph} = 0.21$ Å⁻¹), Equation (7) yields $h_{bb,ph} \approx 7 \cdot h_{bb,xy}$.

The absorption data in Figure 1 indicate that there are significant differences in π -conjugation between the oligo-*p*-phenylene and oligo-*p*-xylylene bridges (see above). Thus it appears reasonable to attribute the differences in $h_{bb,ph}$ and $h_{bb,xy}$ primarily to differences in π -conjugation. This π -conjugation is governed by the overlap between p_z -orbitals on adjacent bridging units, which in turn is a function of the dihedral angle ϕ between them. The angular dependence of h_{bb} is then given by:^[12]

$$h_{bb}(\phi) = h_{bb}(\phi = 0) \cdot [\cos(\phi)^2] \quad (8)$$

A plot of this function is given in the upper panel of Figure 7. The lower panel in Figure 7 shows curves that satisfy the relation $h_{bb,ph}(\phi_{ph-ph}) = x \cdot h_{bb,xy}(\phi_{xy-xy})$, among which the $x = 7$ curve (solid line) represents the most relevant case for our Ru-ph_{*n*}-PTZ and Ru-xy_{*n*}-PTZ systems. There have been several computational studies on the interphenyl torsion angle ϕ_{ph-ph} in oligo-*p*-phenylenes, reporting values that range from 35° to 38° for gas-phase equilibrium structures.^[4c,30] Using the Jaguar 3.5 software package we have been able to reproduce the results from these prior calculations (density functional theory using Becke's three-parameter hybrid functional with Lee, Yang, Parr correlation function B3LYP and a 6-31G* basis set).^[47] Our result obtained for the tri-*p*-phenylene molecule is shown at the lower right bottom of Figure 7. The two phenyl-phenyl torsion angles in this calculated (gas-phase) equilibrium structure are 38°. When applying the exactly same computational method to a tri-*p*-xylylene molecule, one obtains the equilibrium structure shown in the upper left corner of the lower panel in Figure 7. This structure displays xylyl-xylyl torsion angles of 69°. The black circle in the lower panel of Figure 7 marks the point at which the two equilibrium torsion angles ϕ_{ph-ph} and ϕ_{xy-xy} are at the above calculated values (38° and 69°, respectively). We note that this point falls onto the $x = 5$ line. In other words, based on the gas-phase equilibrium structure calculations and Equation (8), one would expect phenyl-phenyl coupling to be 5 times stronger than xylyl-xylyl coupling. The close agreement to the factor of 7 found from experiment supports our analysis of the experimental data in terms of distinct phenyl-phenyl and xylyl-xylyl equilibrium torsion angles. In other words, the experimentally observed differences in long-range charge transfer efficiencies for oligo-*p*-phenylene and oligo-*p*-xylylene bridges can be explained satisfactorily on the sole basis of conformational effects. Other effects, such as possible variations in the tunneling barriers ($\Delta\varepsilon$) as a function of bridge length,^[4c,4d] appear to play a subordinate role. This

is remarkable because in principle the energies of the one-electron oxidized state of oligo-*p*-phenylenes are strongly length-dependent.^[4d]

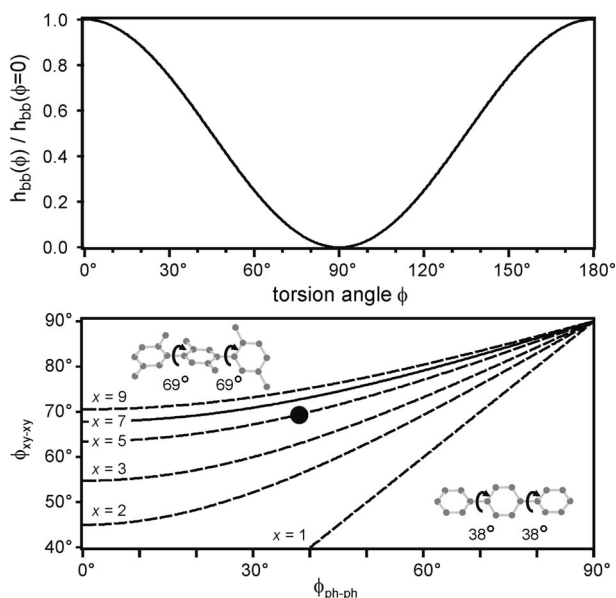


Figure 7. Upper panel: effect of torsion angle (ϕ) on the electronic bridge-bridge coupling (h_{bb}) via p_z -orbital overlap between adjacent bridge units. Lower panel: functions that satisfy the equation $h_{bb,ph}(\phi_{ph-ph}) = x \cdot h_{bb,xy}(\phi_{xy-xy})$, i.e., curves for which phenyl-phenyl coupling is calculated [Equation (8)] to be a factor of x stronger than xylyl-xylyl coupling.

Conclusions

There have been several prior studies that investigated the distance dependence of electron transfer across oligo-*p*-phenylene wires,^[4b–4d,4g] and we have recently reported on the distance dependence of hole tunneling across oligo-*p*-xylene bridges.^[14,23] Since the distance decay constant (β) is a system-specific rather than bridge-specific parameter,^[10,23] we have sought to compare the two types of molecular wires directly by attaching them to the same donor and acceptor. In retrospect, the choice of a phenothiazine/Ru(bpy)₃²⁺ reactant couple turned out to be less than optimal because only two quite different phototriggered charge transfer processes were ultimately amenable to experimental investigation in the oligo-*p*-phenylene and oligo-*p*-xylene bridged systems. That is, PTZ⁺→Ru(bpy)₃⁺ hole tunneling in the Ru-ph_{*n*}-PTZ molecules and Ru(bpy)₃³⁺→PTZ hole tunneling in the Ru-xy_{*n*}-PTZ systems. The barrier heights and driving-forces associated with these two tunneling processes are quite different, but using superexchange theory it is nevertheless possible to extract quantitative information on the relative electronic coupling strengths provided by the oligo-*p*-phenylene and oligo-*p*-xylene bridges.

The key finding is that two adjacent phenyl units are coupled ca. 7 times stronger than two neighboring xylyl units, and this observation can be explained on the sole basis of

conformational effects. Our analysis is based on the evaluation of distance decay constants for long-range charge transfer rates, and our result is in line with those from prior investigations of conformational effects on electronic coupling across substituted and unsubstituted biphenyls.^[12]

Experimental Section

Instrumentation: ¹H-NMR spectra were acquired on a Bruker Avance 400 MHz spectrometer. All chemical shifts are reported in ppm relative to the tetramethylsilane signal. Deuterated solvents were purchased from Sigma Aldrich. The different types of multiplets observed are denoted by the following abbreviations: s (singlet), d (doublet), t (triplet), q (quadruplet), dd (doublet of doublets), ddd (doublet of doublets of doublets), m (multiplet), dm (doublet of multiplets). High resolution mass spectra were recorded on a QSTAR XL (AB/MDS Sciex) spectrometer. Methanol (HPLC grade, VWR) was used to solubilize the samples. Optical absorption spectra were measured on a Cary 5000 UV/Vis/NIR spectrophotometer (Varian), and luminescence experiments were measured on a Horiba Fluorolog-3 instrument. The solvent used for these measurements was acetonitrile of spectrophotometric grade. For luminescence lifetime and transient absorption spectroscopy, 10^{−4} to 2 × 10^{−5} M acetonitrile solutions of the Ru-ph_{*n*}-PTZ molecules were deoxygenated via three subsequent freeze-pump-thaw cycles in home-built quartz cuvettes. Sample excitation occurred using a Quantel Brilliant Nd:YAG laser with an integrated Magic Prism OPO. The detection system was comprised of a Spex 270M monochromator, a Hamamatsu photomultiplier, and a Tektronix TDS 540B oscilloscope. The probe beam used for transient absorption spectroscopy came from a 900-W tungsten lamp. Cyclic voltammetry was performed using a Versastat3–100 Potentiostat equipped with the K0264 Micro-Cell kit from Princeton Applied Research. A silver wire was used as a quasi-reference electrode. The supporting electrolyte was a 0.1 M solution of tetrabutylammonium hexafluorophosphate (Fluka, product No. 86879) in dry acetonitrile (HPLC grade, VWR). The solution was deoxygenated prior to voltammetry sweeps by bubbling nitrogen gas.

Synthetic Protocols: Compound **3** (PTZ-ph₁-TMS): To a double-neck flask containing phenothiazine (**1**) (5 g, 25.2 mmol), (4-bromophenyl)trimethylsilane (**2**) (5.78 g, 25.2 mmol), potassium *tert*-butoxide (4.24 g, 37.8 mmol) and Pd(dba)₂ (dba: dibenzylidene acetone) (290 mg, 504 μmol) were added freshly distilled toluene (125 mL) and a 1 M solution of P(*t*Bu)₃ (*t*Bu: *tert*-butylphosphane) in toluene (0.5 mL, 504 μmol) under a nitrogen atmosphere. The yellow suspension was heated at 60 °C and the reaction followed by TLC until total consumption of the phenothiazine (ca. 2 h). Then the solvent was evaporated under reduced pressure. The crude brown product was then purified by column chromatography on silica gel using a pentane/CH₂Cl₂ (98:2) mixture to elute the N–C coupled product as a slightly yellow solid in 89% yield (7.79 g). ¹H NMR (400 MHz, CDCl₃, 25 °C): δ = 0.39 (s, 9 H, SiMe₃), 6.30 (dd, J = 8.0, 0.9 Hz, 2 H, PTZ), 6.86 (m, 4 H, PTZ), 7.05 (dd, J = 7.2, 1.5 Hz, 2 H, PTZ), 7.12 (d, J = 8.4 Hz, 2 H, Ph), 7.89 (d, J = 8.4 Hz, 2 H, Ph) ppm.

Compound 4 (PTZ-ph₁-I): To a double-neck flask containing a yellow suspension of the trimethylsilyl-protected compound **3** (1 g, 2.9 mmol) in a mixture of CH₂Cl₂/CH₃CN (1:3) at 0 °C was added a solution of ICl (934 mg, 5.8 mmol) in CH₂Cl₂ (25 mL) under a nitrogen atmosphere. The resulting dark orange suspension was

warmed to ca. 20 °C and stirred during 20 h at this temperature. The reaction was followed by NMR until disappearance of the TMS singlet. Then, the mixture was hydrolyzed using aqueous Na₂S₂O₃ solution and extracted by CH₂Cl₂. The combined organic phases were concentrated under reduced pressure. The crude brown product was then purified by column chromatography on silica and eluted by a pentane/CH₂Cl₂ (98:2) mixture to give the desired product as a yellow solid in 99% yield (1.15 g). ¹H NMR (400 MHz, CDCl₃, 25 °C): δ = 6.30 (dd, *J* = 8.0, 1.50 Hz, 2 H, 2 H, PTZ), 6.86 (m, 4 H, PTZ), 7.05 (dd, *J* = 7.2, 2.0 Hz, 2 H, PTZ), 7.11 (d, *J* = 8.4 Hz, 2 H, Ph), 7.89 (d, *J* = 8.4 Hz, 2 H, Ph) ppm.

Ligand 6 (PTZ-ph₁-bpy): To a stirred and deoxygenated suspension of iodo compound **4** (1.00 g, 2.5 mmol), 5-(tri-*n*-butylstannyl)-2,2'-bipyridine (**5**) (1.44 g, 3.2 mmol) in *m*-xylene under nitrogen atmosphere was added Pd(PPh₃)₄ (Ph: phenyl) (144 mg, 125 μmol). The yellow suspension was deoxygenated for an additional 10 min by bubbling nitrogen gas and then heated to 140 °C during 48 h. After cooling to room temperature, the solvent was evaporated under reduced pressure. The dark brown remaining solid was then purified by two successive column chromatographies on silica gel, first using a CH₂Cl₂/CH₃OH (98:2) eluent mixture and then a pentane/ethyl acetate eluent mixture (80:20). This gave the desired coupling product in the form of an orange oil in 54% yield (0.58 g). ¹H NMR (400 MHz, CDCl₃, 25 °C): δ = 6.39 (dd, *J* = 8.0, 1.2 Hz, 2 H, PTZ), 6.86 (ddd, *J* = 7.6, 7.6, 1.2 Hz, 2 H, PTZ), 6.93 (ddd, *J* = 7.6, 7.6, 2.0 Hz, 2 H, PTZ), 7.08 (dd, *J* = 7.6, 1.6 Hz, 2 H, PTZ), 7.34 (ddd, *J* = 7.6, 4.8, 1.2 Hz, 1 H, bpy), 7.50 (d, *J* = 8.4 Hz, 1 H, Ph), 7.85 (m, 1 H, bpy), 7.86 (d, *J* = 8.4 Hz, 2 H, Ph), 8.09 (dd, *J* = 8.4, 2.4 Hz, 1 H, bpy), 8.47 (ddd, *J* = 7.6, 1.2, 1.2 Hz, 1 H, bpy), 8.53 (dd, *J* = 8.0, 0.8 Hz, 1 H, bpy), 8.72 (dm, *J* = 4.8 Hz, 1 H, bpy), 9.00 (d, *J* = 2.4 Hz, 1 H, bpy) ppm. ESI-MS: *m/z* calcd. for protonated PTZ-ph₁-bpy: 430.5; found 430.3.

Ru-ph₁-PTZ: A solution of PTZ-ph₁-bpy ligand (100 mg, 233 μmol) and Ru(bpy)₂Cl₂·2H₂O (128 mg, 233 μmol) in a mixture of CHCl₃/C₂H₅OH (2:8) was heated to reflux under nitrogen atmosphere overnight. After solvent evaporation under reduced pressure, the remaining dark solid was purified twice by column chromatography on silica: first using a CH₂Cl₂/CH₃OH eluent mixture (98:2), then using an eluent mixture comprised of CH₃CN and saturated aqueous KNO₃ (99:1) to afford the nitrate salt of the desired complex. Nitrate to hexafluorophosphate anion exchange was achieved by precipitation of the orange complex from an aqueous solution using saturated aqueous KPF₆. The yield was 68% (153 mg). ¹H NMR (400 MHz, CD₃CN, 25 °C): δ = 6.66 (dd, *J* = 7.6, 1.2 Hz, 2 H, PTZ), 7.02 (ddd, *J* = 7.2, 7.2, 1.2 Hz, 2 H, PTZ), 7.09 (ddd, *J* = 7.6, 7.2, 2.0 Hz, 2 H, PTZ), 7.23 (dd, *J* = 7.6, 1.6 Hz, 2 H, PTZ), 7.26 (dm, *J* = 8.8 Hz, 2 H, Ph), 7.41 (m, 5 H), 7.50 (dm, *J* = 8.4 Hz, 1 H, bpy), 7.74 (m, 2 H), 7.77 (dm, *J* = 5.6 Hz, 1 H, bpy), 7.80 (dm, *J* = 5.6 Hz, 1 H, bpy), 7.85 (dm, *J* = 5.6 Hz, 1 H, bpy), 7.88 (dm, *J* = 5.6 Hz, 1 H, bpy), 8.07 (m, 5 H), 8.32 (dd, *J* = 8.8, 2.4 Hz, 1 H, bpy), 8.56 (m, 5 H), 8.60 (dm, *J* = 8.8 Hz, 1 H, bpy) ppm. ESI-MS: *m/z* calcd. for the Ru-ph₁-PTZ dication: 421.5853; found 421.5852. C₄₈H₃₅F₁₂N₇P₂RuS·0.2CHCl₃: calcd. C 49.80, H 3.05, N 8.42; found C 49.84, H 3.21, N 8.18.

4-Bromo-4'-trimethylsilyl-1,1'-biphenyl (7): To a stirred solution of 4,4'-dibromo-1,1'-biphenyl (10.0 g, 32.1 mmol) in dry ethyl ether cooled to -78 °C under nitrogen atmosphere, 1.6 M solution of *n*-butyllithium in hexane (41.7 mmol, 26.0 mL) was added dropwise via syringe. After 1 h, chlorotrimethylsilane (41.7 mmol, 5.3 mL) was added. After stirring for an additional 30 min at -78 °C, the reaction mixture was warmed to room temperature. Following addition of water, the mixture was extracted with dichloromethane.

The combined organic phases were dried, and the solvent was evaporated under reduced pressure. The remaining yellow oil was purified subsequently by column chromatography on silica gel using pentane as the eluent. The product yield was 88% (8.65 g). ¹H NMR (400 MHz, CDCl₃, 25 °C): δ = 0.32 (s, 9 H, SiMe₃), 7.41–7.48 (m, 2 H, Ph), 7.55–7.63 (m, 6 H, Ph) ppm.

PTZ-ph₂-TMS 8: To a two-neck flask containing phenothiazine (**1**) (5 g, 25.2 mmol), 4-bromo-4'-trimethylsilyl-1,1'-biphenyl (**7**) (7.70 g, 25.2 mmol), potassium tertbutanolate (4.24 g, 37.8 mmol) and Pd(dba)₂ (290 mg, 504 μmol) were added freshly distilled toluene (125 mL), and a 1 M solution of P(*t*Bu)₃ in toluene (0.5 mL, 504 μmol) under a nitrogen atmosphere. The yellow suspension was heated at 60 °C, and the reaction was followed by TLC until complete disappearance of **1**. Then the solvent was evaporated under reduced pressure. Purification of the crude brown product occurred by column chromatography on silica gel using a pentane/CH₂Cl₂ (98:2) eluent mixture. The product was obtained in 62% yield in the form of a slightly yellow solid. ¹H NMR (400 MHz, CDCl₃, 25 °C): δ = 0.34 (s, 9 H, SiMe₃), 6.34 (dd, *J* = 8.0, 1.2 Hz, 2 H, PTZ), 6.86 (m, 4 H, PTZ), 7.05 (dd, *J* = 7.2, 1.6 Hz, 2 H, PTZ), 7.45 (d, *J* = 8.4 Hz, 2 H, Ph), 7.66 (s, 4 H, Ph), 7.81 (d, *J* = 8.4 Hz, 2 H, Ph) ppm.

PTZ-ph₂-I 9: To a suspension of PTZ-ph₂-TMS (**8**) (2.0 g, 4.7 mmol) in a mixture of CH₂Cl₂/CH₃CN (1:3) at 0 °C was added a solution of ICl (1.53 g, 9.4 mmol) in CH₂Cl₂ (25 mL) under a nitrogen atmosphere. The resulting dark orange suspension was warmed to ca. 20 °C and stirred at this temperature. The reaction was followed by ¹H-NMR until disappearance of the characteristic TMS singlet (ca. 20 h). Then the mixture was hydrolyzed using aqueous Na₂S₂O₃ solution and extracted by CH₂Cl₂. After solvent evaporation, the crude brown product was purified by column chromatography on silica gel using a pentane/CH₂Cl₂ (98:2) mixture as an eluent. This afforded the product in 80% yield as a yellow solid (1.83 g). ¹H NMR (400 MHz, CDCl₃, 25 °C): δ = 6.34 (dd, *J* = 8.0, 1.2 Hz, 2 H, PTZ), 6.83–6.92 (m, 4 H, PTZ), 7.05 (dd, *J* = 7.2, 1.6 Hz, 2 H, PTZ), 7.40 (d, *J* = 8.4 Hz, 2 H, Ph), 7.44 (d, *J* = 8.4 Hz, 2 H, Ph), 7.75 (d, *J* = 8.4 Hz, 2 H, Ph), 7.81 (d, *J* = 8.4 Hz, 2 H, Ph) ppm.

Ligand 10 (PTZ-ph₂-bpy): To a deoxygenated suspension of PTZ-ph₂-TMS (**9**) (1.00 g, 2.1 mmol), 5-(tri-*n*-butylstannyl)-2,2'-bipyridine (**5**) (1.21 g, 2.7 mmol) in 20 mL *m*-xylene under nitrogen atmosphere was added Pd(PPh₃)₄ (121 mg, 105 μmol). The reaction mixture was degassed for an additional 10 min by bubbling nitrogen gas prior to heating to 140 °C during 48 h. After cooling to room temperature and solvent evaporation under reduced pressure, the remaining dark brown solid was purified by two successive column chromatographies on a silica gel stationary phase: first with a CH₂Cl₂/MeOH (98:2) mixture, then with a pentane/ethyl acetate (80:20) eluent mixture. This afforded the desired coupling product in 40% yield as an orange oil (425 mg). ¹H NMR (400 MHz, CDCl₃, 25 °C): δ = 6.37 (dd, *J* = 8.0, 1.2 Hz, 2 H, PTZ), 6.85 (ddd, *J* = 7.6, 7.6, 1.2 Hz, 2 H, PTZ), 6.91 (ddd, *J* = 7.6, 7.6, 2.0 Hz, 2 H, PTZ), 7.06 (dd, *J* = 7.6, 1.6 Hz, 2 H, PTZ), 7.34 (ddd, *J* = 7.6, 4.8, 1.2 Hz, 1 H, bpy), 7.49 (dm, *J* = 8.4 Hz, 2 H, Ph), 7.80 (s, 4 H, Ph); 7.85 (dm, *J* = 8.4 Hz, 2 H, Ph), 7.87 (m, 1 H, bpy), 8.10 (dd, *J* = 8.4, 2.4 Hz, 1 H, bpy), 8.52 (ddd, *J* = 7.6, 1.2, 1.2 Hz, 1 H, bpy), 8.72 (dd, *J* = 8.0, 0.8 Hz, 1 H, bpy), 9.01 (dm, *J* = 2.4 Hz, 1 H, bpy) ppm. ESI-MS: *m/z* calcd. for protonated PTZ-ph₂-bpy: 506.6; found 506.5.

Ru-ph₂-PTZ: A solution of PTZ-ph₂-bpy (**10**) (100 mg, 198 μmol) and Ru(bpy)₂Cl₂·2H₂O (109 mg, 198 μmol) in a mixture of CHCl₃/C₂H₅OH (2:8) was heated to reflux under nitrogen atmosphere

overnight. After solvent evaporation, the remaining dark solid was purified by two successive column chromatographies on silica gel. The first used a CH₂Cl₂/CH₃OH mixture (98:2), the second a mixture of CH₃CN and saturated aqueous KNO₃ (99:1) to elute the product. NO₃⁻ to PF₆⁻ anion exchange occurred as described above for Ru-ph₁-PTZ. Ru-ph₂-PTZ was isolated as a deep orange solid in 65% yield (134 mg). ¹H NMR (400 MHz, CD₃CN, 25 °C): δ = 6.66 (dd, *J* = 7.6, 1.2 Hz, 2 H, PTZ), 7.02 (ddd, *J* = 7.2, 7.2, 1.2 Hz, 2 H, PTZ), 7.09 (ddd, *J* = 7.6, 7.2 Hz, 2 H, PTZ), 7.23 (dd, *J* = 7.6, 1.6 Hz, 2 H, PTZ), 7.26 (dm, *J* = 8.8 Hz, 2 H, Ph), 7.43 (m, 6 H), 7.54 (dd, *J* = 8.8, 2.0 Hz, 2 H, Ph), 7.77 (m, 5 H), 7.84 (dm, *J* = 4.8 Hz, 1 H, bpy), 7.87 (dm, *J* = 2.0 Hz, 1 H, bpy), 7.90 (dm, *J* = 6.0 Hz, 1 H, bpy), 8.08 (m, 5 H), 8.37 (dm, *J* = 8.4 Hz, 1 H, bpy), 8.57 (m, 5 H), 8.63 (dm, *J* = 8.0 Hz, 1 H, bpy) ppm. ESI-MS: *m/z* calcd. for the Ru-ph₂-PTZ dication: 459.6010; found 459.6012. C₅₄H₃₉F₁₂N₇P₂RuS·2.0H₂O: calcd. C 52.09, H 3.48, N 7.87; found C 52.33, H 3.43, N 7.73.

PTZ-ph₃-TMS 12: To a stirred and deoxygenated suspension of PTZ-ph₂-I (**9**) (1.00 g, 2.1 mmol), 4-(trimethylsilyl)phenylboronic acid **11** (447 mg, 2.3 mmol), and Na₂CO₃ (666 mg, 6.3 mmol) in a mixture of toluene/ethanol/water (85:10:5) under nitrogen atmosphere was added Pd(PPh₃)₄ (48 mg, 42 μmol). The yellow suspension was degassed for an additional 10 min and then heated to reflux overnight. After cooling to room temperature, the mixture was extracted with CH₂Cl₂, and the combined organic phases were evaporated to dryness under reduced pressure. The resulting dark brown solid was purified by column chromatography on silica gel using a CH₂Cl₂/CH₃OH (98:2) mixture to elute the product. The yield was 80% (0.84 g). ¹H NMR (400 MHz, CDCl₃, 25 °C): δ = 0.32 (s, 9 H, SiMe₃), 6.34 (dd, *J* = 8.0, 1.2 Hz, 2 H, PTZ), 6.82–6.92 (m, 4 H, PTZ), 7.05 (dd, *J* = 7.2, 1.2 Hz, 2 H, PTZ), 7.47 (d, *J* = 8.4 Hz, 2 H, Ph), 7.65 (m, 4 H, Ph), 7.74 (m, 4 H, Ph), 7.81 (d, *J* = 8.8 Hz, 2 H, Ph) ppm.

PTZ-ph₃-I 13: To a suspension of PTZ-ph₂-TMS (**12**) (2.0 g, 4.0 mmol) in a mixture of CH₂Cl₂/CH₃CN (1:3) at 0 °C was added a solution of ICl (1.30 g, 8.0 mmol) in CH₂Cl₂ (25 mL) under a nitrogen atmosphere. The dark orange suspension was warmed to room temperature and stirred during 20 h at this temperature. Then, aqueous Na₂S₂O₃ solution was added, and the biphasic mixture was extracted with CH₂Cl₂. The combined organic phases were dried prior to solvent evaporation. The resulting crude brown product was purified by column chromatography on silica gel, using a pentane/CH₂Cl₂ (98:2) mixture to elute the product in 73% yield (1.62 g). ¹H NMR (400 MHz, CDCl₃, 25 °C): δ = 6.35 (dd, *J* = 8.0, 1.20 Hz, 2 H, PTZ), 6.82–6.92 (m, 4 H, PTZ), 7.06 (dd, *J* = 7.2, 1.6 Hz, 2 H, PTZ), 7.41 (d, *J* = 8.4 Hz, 2 H, Ph), 7.47 (d, *J* = 8.4 Hz, 2 H, Ph), 7.68 (d, *J* = 8.4 Hz, 2 H, Ph), 7.75 (d, *J* = 8.8 Hz, 2 H, Ph), 7.80 (d, *J* = 8.4 Hz, 2 H, Ph), 7.84 (d, *J* = 6.8 Hz, 2 H, Ph) ppm.

PTZ-ph₃-bpy 14: PTZ-ph₃-I **13** (1.0 g, 1.8 mmol) and 5-(tri-*n*-butylstannyl)-2,2'-bipyridine (**5**) (1.05 g, 2.3 mmol) were suspended together in 20 mL *m*-xylene. After deoxygenating by bubbling nitrogen gas, Pd(PPh₃)₄ (104 mg, 90 μmol) catalyst was added, then the solution was deoxygenated for an additional 10 min. After heating to 140 °C during 48 h, the reaction mixture was cooled to room temperature and the solvent was evaporated under reduced pressure. The remaining dark brown solid was purified by two successive column chromatographies on silica gel, first with an eluent comprised of a CH₂Cl₂/CH₃OH (98:2) mixture, second with an eluent comprised of pentane/ethyl acetate (80:20). This afforded the coupling product in 23% yield in the form of an orange solid (241 mg). ¹H NMR (400 MHz, CDCl₃, 25 °C): δ = 6.35 (dd, *J* = 8.4, 1.2 Hz,

2 H, PTZ), 6.85 (ddd, *J* = 7.2, 7.2, 1.2 Hz, 2 H, PTZ), 6.90 (ddd, *J* = 7.6, 7.2, 2.0 Hz, 2 H, PTZ), 7.05 (dd, *J* = 7.6, 1.6 Hz, 2 H, PTZ), 7.34 (ddd, *J* = 7.6, 4.8, 1.2 Hz, 1 H, bpy), 7.48 (dm, *J* = 8.8 Hz, 2 H, Ph), 7.79 (s, 8 H, Ph), 7.87 (dm, *J* = 8.8 Hz, 2 H, Ph), 7.87 (m, 1 H, bpy), 8.10 (dd, *J* = 8.0, 2.0 Hz, 1 H, bpy), 8.47 (dm, *J* = 8.0 Hz, 1 H, 8.47), 8.52 (dm, *J* = 8.4 Hz, 1 H, bpy), 8.73 (d, *J* = 4.0 Hz, 1 H, bpy), 9.00 (dm, *J* = 2.4 Hz, 1 H, bpy) ppm. ESI-MS: *m/z* calcd. for protonated PTZ-ph₃-bpy: 582.7; found 582.5.

Ru-ph₃-PTZ: A solution of ligand **14** (100 mg, 233 μmol) and Ru(bpy)₂Cl₂·2H₂O (128 mg, 233 μmol) in a mixture of CHCl₃/C₂H₅OH (2:8) was heated to reflux under nitrogen atmosphere overnight. The resulting orange solution was evaporated to dryness under reduced pressure, and the remaining dark red solid was purified by two subsequent column chromatographies on a silica gel stationary phase. The eluent for the first column was a CH₂Cl₂/CH₃OH mixture (98:2), whereas for the second column a saturated aqueous CH₃CN/KNO₃ mixture (99:1) was employed. Anion exchange from nitrate to hexafluorophosphate was accomplished as described above for Ru-ph₁-PTZ. The Ru-ph₃-PTZ product was obtained in 65% yield (84 mg). ¹H NMR (400 MHz, CD₃CN, 25 °C): δ = 6.39 (dd, *J* = 8.0, 1.2 Hz, 2 H, PTZ), 6.89 (ddd, *J* = 7.2, 7.2, 1.2 Hz, 2 H, PTZ), 6.96 (ddd, *J* = 7.6, 7.2, 2.0 Hz, 2 H, PTZ), 7.09 (dd, *J* = 7.6, 1.6 Hz, 2 H, PTZ), 7.44 (m, 8 H), 7.53 (dm, *J* = 8.4 Hz, 2 H, Ph), 7.80 (m, 10 H), 7.87 (d, *J* = 1.6 Hz, 1 H, bpy), 7.92 (m, 4 H), 8.08 (m, 6 H), 8.37 (dm, *J* = 8.4 Hz, 1 H, bpy), 8.58 (m, 6 H), 8.62 (dm, *J* = 8.4 Hz, 1 H, bpy) ppm. ESI-MS: *m/z* calcd. for the Ru-ph₃-PTZ dication: 497.6166; found 497.6164. C₆₀H₄₃F₁₂N₇P₂RuS·2C₄H₈O₂: calcd. C 55.89, H 4.07, N 6.71; found C 55.61, H 3.74, N 6.53.

Acknowledgments

This research was sponsored by the Swiss National Science Foundation (grant number PP002-110611). The Société Académique de Genève and the Fondation Ernst & Lucie Schmidheiny are acknowledged for additional financial support.

- [1] a) W. B. Davis, W. A. Svec, M. A. Ratner, M. R. Wasielewski, *Nature* **1998**, *396*, 60–63; b) R. Huber, M. T. González, S. Wu, M. Langer, S. Grunder, V. Horhoiu, M. Mayor, M. R. Bryce, C. S. Wang, R. Jitchati, C. Schönenberger, M. Calame, *J. Am. Chem. Soc.* **2008**, *130*, 1080–1084; c) G. de la Torre, F. Giacalone, J. L. Segura, N. Martín, D. M. Guldi, *Chem. Eur. J.* **2005**, *11*, 1267–1280; d) H. D. Sikes, J. F. Smalley, S. P. Dudek, A. R. Cook, M. D. Newton, C. E. D. Chidsey, S. W. Feldberg, *Science* **2001**, *291*, 1519–1523; e) F. Giacalone, J. L. Segura, N. Martín, D. M. Guldi, *J. Am. Chem. Soc.* **2004**, *126*, 5340–5341; f) R. Hoofman, M. P. de Haas, L. D. A. Siebbeles, J. M. Warman, *Nature* **1998**, *392*, 54–56.
- [2] a) J. Fortage, E. Göransson, E. Blart, H. C. Becker, L. Hammarström, F. Odobel, *Chem. Commun.* **2007**, 4629–4631; b) M. Wielopolski, C. Atienza, T. Clark, D. M. Guldi, N. Martín, *Chem. Eur. J.* **2008**, *14*, 6379–6390; c) L. A. Bumm, J. J. Arnold, M. T. Cygan, T. D. Dunbar, T. P. Burgin, L. Jones, D. L. Allara, J. M. Tour, P. S. Weiss, *Science* **1996**, *271*, 1705–1707; d) M. P. Eng, J. Mårtensson, B. Albinsson, *Chem. Eur. J.* **2008**, *14*, 2819–2826; e) B. Albinsson, M. P. Eng, K. Pettersson, M. U. Winters, *Phys. Chem. Chem. Phys.* **2007**, *9*, 5847–5864; f) S. Creager, C. J. Yu, C. Bamdad, S. O'Connor, T. MacLean, E. Lam, Y. Chong, G. T. Olsen, J. Y. Luo, M. Gozin, J. F. Kayyem, *J. Am. Chem. Soc.* **1999**, *121*, 1059–1064.
- [3] a) R. H. Goldsmith, L. E. Sinks, R. F. Kelley, L. J. Betzen, W. H. Liu, E. A. Weiss, M. A. Ratner, M. R. Wasielewski, *Proc.*

- Natl. Acad. Sci. USA* **2005**, *102*, 3540–3545; b) C. Atienza-Castellanos, M. Wielopolski, D. M. Guldi, C. van der Pol, M. R. Bryce, S. Filippone, N. Martín, *Chem. Commun.* **2007**, 5164–5166; c) R. H. Goldsmith, O. DeLeon, T. M. Wilson, D. Finkelstein-Shapiro, M. A. Ratner, M. R. Wasielewski, *J. Phys. Chem. A* **2008**, *112*, 4410–4414.
- [4] a) F. Barigelletti, L. Flamigni, *Chem. Soc. Rev.* **2000**, *29*, 1–12; b) M. T. Indelli, C. Chiorboli, L. Flamigni, L. De Cola, F. Scandola, *Inorg. Chem.* **2007**, *46*, 5630–5641; c) E. A. Weiss, M. J. Ahrens, L. E. Sinks, A. V. Gusev, M. A. Ratner, M. R. Wasielewski, *J. Am. Chem. Soc.* **2004**, *126*, 5577–5584; d) E. A. Weiss, M. J. Tauber, R. F. Kelley, M. J. Ahrens, M. A. Ratner, M. R. Wasielewski, *J. Am. Chem. Soc.* **2005**, *127*, 11842–11850; e) M. T. Indelli, F. Scandola, L. Flamigni, J.-P. Collin, J.-P. Sauvage, A. Sour, *Inorg. Chem.* **1997**, *36*, 4247–4250; f) E. Lörtscher, M. Elbing, M. Tschudy, C. von Hänisch, H. B. Weber, M. Mayor, H. Riel, *ChemPhysChem* **2008**, *9*, 2252–2258; g) A. Helms, D. Heiler, G. McLendon, *J. Am. Chem. Soc.* **1992**, *114*, 6227–6238.
- [5] a) K. Weber, L. Hockett, S. Creager, *J. Phys. Chem. B* **1997**, *101*, 8286–8291; b) H. Oevering, M. N. Paddon-Row, M. Heppener, A. M. Oliver, E. Cotsaris, J. W. Verhoeven, N. S. Hush, *J. Am. Chem. Soc.* **1987**, *109*, 3258–3269.
- [6] a) K. S. Schanze, L. A. Cabana, *J. Phys. Chem.* **1990**, *94*, 2740–2743; b) K. S. Schanze, K. Sauer, *J. Am. Chem. Soc.* **1988**, *110*, 1180–1186; c) R. A. Malak, Z. N. Gao, J. F. Wishart, S. S. Isied, *J. Am. Chem. Soc.* **2004**, *126*, 13888–13889; d) S. A. Seron, W. S. Aldridge, C. N. Fleming, R. M. Danell, M. H. Baik, M. Sykora, D. M. Dattelbaum, T. J. Meyer, *J. Am. Chem. Soc.* **2004**, *126*, 14506–14514; e) Y. T. Long, E. Abu-Rhayem, H. B. Kraatz, *Chem. Eur. J.* **2005**, *11*, 5186–5194.
- [7] a) H. B. Gray, J. R. Winkler, *Proc. Natl. Acad. Sci. USA* **2005**, *102*, 3534–3539; b) C. C. Moser, J. M. Keske, K. Warncke, R. S. Farid, P. L. Dutton, *Nature* **1992**, *355*, 796–802; c) H. B. Gray, J. R. Winkler, *Annu. Rev. Biochem.* **1996**, *65*, 537–561.
- [8] a) B. Paulson, K. Pramod, P. Eaton, G. Closs, J. R. Miller, *J. Phys. Chem.* **1993**, *97*, 13042–13045; b) G. L. Closs, L. T. Calcaterra, N. J. Green, K. W. Penfield, J. R. Miller, *J. Phys. Chem.* **1986**, *90*, 3673–3683.
- [9] a) T. Guarr, M. McGuire, S. Strauch, G. McLendon, *J. Am. Chem. Soc.* **1983**, *105*, 616–618; b) J. R. Miller, J. V. Beitz, R. K. Huddleston, *J. Am. Chem. Soc.* **1984**, *106*, 5057–5068; c) A. Ponce, H. B. Gray, J. R. Winkler, *J. Am. Chem. Soc.* **2000**, *122*, 8187–8191; d) O. S. Wenger, B. S. Leigh, R. M. Villahermosa, H. B. Gray, J. R. Winkler, *Science* **2005**, *307*, 99–102; e) O. S. Wenger, H. B. Gray, J. R. Winkler, *Chimia* **2005**, *59*, 94–96.
- [10] a) F. D. Lewis, J. Q. Liu, W. Weigel, W. Rettig, I. V. Kurnikov, D. N. Beratan, *Proc. Natl. Acad. Sci. USA* **2002**, *99*, 12536–12541; b) K. Kilså, J. Kajanus, A. N. Macpherson, J. Martensson, B. Albinsson, *J. Am. Chem. Soc.* **2001**, *123*, 3069–3080; c) M. P. Eng, B. Albinsson, *Angew. Chem. Int. Ed.* **2006**, *45*, 5626–5629; d) O. S. Wenger, *Chimia* **2007**, *61*, 823–825; e) B. Kim, J. M. Beebe, Y. Jun, X. Y. Zhu, C. D. Frisbie, *J. Am. Chem. Soc.* **2006**, *128*, 4970–4971.
- [11] A. Helms, D. Heiler, G. McLendon, *J. Am. Chem. Soc.* **1991**, *113*, 4325–4327.
- [12] a) A. C. Benniston, A. Harriman, P. Y. Li, P. V. Patel, C. A. Sams, *Phys. Chem. Chem. Phys.* **2005**, *7*, 3677–3679; b) A. C. Benniston, A. Harriman, *Chem. Soc. Rev.* **2006**, *35*, 169–179.
- [13] M. Maus, W. Rettig, G. Jonusauskas, R. Lapouyade, C. Rullière, *J. Phys. Chem. A* **1998**, *102*, 7393–7405.
- [14] D. Hanss, O. S. Wenger, *Inorg. Chem.* **2008**, *47*, 9081–9084.
- [15] a) V. Hensel, A. D. Schlüter, *Liebigs Ann./Recueil* **1997**, 303–309; b) V. Hensel, K. Lutzow, J. Jacob, K. Gessler, W. Saenger, A. D. Schlüter, *Angew. Chem. Int. Ed. Engl.* **1997**, *36*, 2654–2656.
- [16] a) J. C. Freys, D. Hanss, M. E. Walther, O. S. Wenger, *Chimia* **2009**, *63*, 49–53; b) D. Hanss, O. S. Wenger, *Inorg. Chim. Acta* **2009**, *362*, 3415–3420.
- [17] S. L. Mecklenburg, D. G. McCafferty, J. R. Schoonover, B. M. Peek, B. W. Erickson, T. J. Meyer, *Inorg. Chem.* **1994**, *33*, 2974–2983.
- [18] S. A. Alkaitis, G. Beck, M. Grätzel, *J. Am. Chem. Soc.* **1975**, *97*, 5723–5729.
- [19] B. V. Bergeron, G. J. Meyer, *J. Phys. Chem. B* **2003**, *107*, 245–254.
- [20] G. Ajayakumar, K. Sreenath, K. R. Gopidas, *Dalton Trans.* **2009**, 1180–1186.
- [21] L. D. Margerum, T. J. Meyer, R. W. Murray, *J. Phys. Chem.* **1986**, *90*, 2696–2702.
- [22] O. S. Wenger, *Coord. Chem. Rev.* **2009**, *253*, 1439–1457.
- [23] a) D. Hanss, O. S. Wenger, *Inorg. Chem.* **2009**, *48*, 671–680; b) M. E. Walther, O. S. Wenger, *ChemPhysChem* **2009**, *10*, 1203–1206.
- [24] M. E. Walther, O. S. Wenger, *Dalton Trans.* **2008**, 6311–6318.
- [25] a) C. Brotschi, G. Mathis, C. J. Leumann, *Chem. Eur. J.* **2005**, *11*, 1911–1923; b) T. Haino, H. Araki, Y. Yamanaka, Y. Fukazawa, *Tetrahedron Lett.* **2001**, *42*, 3203–3206.
- [26] T. Okamoto, M. Kuratsu, M. Kozaki, K. Hirotsu, A. Ichimura, T. Matsushita, K. Okada, *Org. Lett.* **2004**, *6*, 3493–3496.
- [27] M. Querol, B. Bozic, N. Salluce, P. Belser, *Polyhedron* **2003**, *22*, 655–664.
- [28] B. P. Sullivan, D. J. Salmon, T. J. Meyer, *Inorg. Chem.* **1978**, *17*, 3334–3341.
- [29] a) S. Welter, F. Lafalet, E. Cecchetto, F. Vergeer, L. De Cola, *ChemPhysChem* **2005**, *6*, 2417–2427; b) F. Lafalet, S. Welter, Z. Popovic, L. De Cola, *J. Mater. Chem.* **2005**, *15*, 2820–2828.
- [30] a) S. Bouzakraoui, S. M. Bouzzine, M. Bouachrine, M. Hamidi, *J. Mol. Struct.* **2005**, *725*, 39–44; b) V. Lukeš, A. J. A. Aquino, H. Lischka, H. F. Kauffmann, *J. Phys. Chem. B* **2007**, *111*, 7954–7962; c) C. Grave, C. Risko, A. Shaporenko, Y. L. Wang, C. Nuckolls, M. A. Ratner, M. A. Rampi, M. Zharnikov, *Adv. Funct. Mater.* **2007**, *17*, 3816–3828.
- [31] a) S. L. Larson, C. M. Elliott, D. F. Kelley, *Inorg. Chem.* **1996**, *35*, 2070–2076; b) L. F. Cooley, S. L. Larson, C. M. Elliott, D. F. Kelley, *J. Phys. Chem.* **1991**, *95*, 10694–10700.
- [32] M. Borgström, O. Johansson, R. Lomoth, H. B. Baudin, S. Wallin, L. C. Sun, B. Åkermark, L. Hammarström, *Inorg. Chem.* **2003**, *42*, 5173–5184.
- [33] D. M. Roundhill, *Photochemistry and Photophysics of Metal Complexes*, Plenum Press, New York, **1994**.
- [34] Calculated based on the two approximations $E(\text{Ru}\{\text{bpy}\}_3^{*2+/+}) \approx E(\text{Ru}\{\text{bpy}\}_3^{2+/+}) + E_{00}$ and $-\Delta G_{ET} \approx e[E(\text{Ru}\{\text{bpy}\}_3^{*2+/+}) - E(\text{PTZ}^{+/0})]$, i.e., without Coulombic correction term and Born solvation term.
- [35] A. Yoshimura, M. Z. Hoffman, H. Sun, *J. Photochem. Photobiol. A: Chem.* **1993**, *70*, 29–33.
- [36] Q. G. Mulazzani, S. Emmi, P. G. Fuoichi, M. Z. Hoffman, M. Venturi, *J. Am. Chem. Soc.* **1978**, *100*, 981–983.
- [37] C. P. Anderson, D. J. Salmon, T. J. Meyer, R. C. Young, *J. Am. Chem. Soc.* **1977**, *99*, 1980–1982.
- [38] P. W. Atkins, *Physical Chemistry, 8th edition*, Oxford University Press, **2006**.
- [39] a) P. Y. Chen, T. D. Westmoreland, E. Danielson, K. S. Schanze, D. Anthon, P. E. Neveux, T. J. Meyer, *Inorg. Chem.* **1987**, *26*, 1116–1126; b) K. S. Schanze, D. B. MacQueen, T. A. Perkins, L. A. Cabana, *Coord. Chem. Rev.* **1993**, *122*, 63–89.
- [40] Z. E. X. Dance, M. J. Ahrens, A. M. Vega, A. B. Ricks, D. W. McCamant, M. A. Ratner, M. R. Wasielewski, *J. Am. Chem. Soc.* **2008**, *130*, 830–831.
- [41] P. P. Edwards, H. B. Gray, M. T. J. Lodge, R. J. P. Williams, *Angew. Chem. Int. Ed.* **2008**, *47*, 6758–6765.
- [42] M. J. Bjerrum, D. R. Casimiro, I. J. Chang, A. J. DiBilio, H. B. Gray, M. G. Hill, R. Langen, G. A. Mines, L. K. Skov, J. R. Winkler, D. S. Wuttke, *J. Bioenerg. Biomembr.* **1995**, *27*, 295–302.
- [43] We note that even faster laser equipment and a diffusion-limited time resolution of ca. 1 ns is likely to be insufficient to investigate the $\text{PTZ} \rightarrow \text{Ru}^{\text{III}}$ charge transfer kinetics in the Ru

- ph₁-PTZ molecule. From a fit to the Ru-xy_n-PTZ data we determine $k_0 = 3 \times 10^{10} \text{ s}^{-1}$ for the PTZ/Ru(bpy)₃³⁺ couple. Since for $r_{DA} = 19.2 \text{ \AA}$ (Ru-ph₃-PTZ) $k_{\text{tunneling}} \geq 10^8 \text{ s}^{-1}$, and thus $\beta \leq 0.43 \text{ \AA}^{-1}$ for this process. Consequently, for the Ru-ph₁-PTZ system the tunneling rate is expected to be $\geq 4.9 \times 10^9 \text{ s}^{-1}$.
- [44] K. Ishiguro, T. Nakano, H. Shibata, Y. Sawaki, *J. Am. Chem. Soc.* **1996**, *118*, 7255–7264.
- [45] H. M. McConnell, *J. Chem. Phys.* **1961**, *35*, 508–515.
- [46] R. A. Marcus, N. Sutin, *Biochim. Biophys. Acta* **1985**, *811*, 265–322.
- [47] a) A. D. Becke, *J. Chem. Phys.* **1993**, *98*, 1372–1377; b) C. T. Lee, W. T. Yang, R. G. Parr, *Phys. Rev. B* **1988**, *37*, 785–789.

Received: May 1, 2009

Published Online: July 23, 2009